Nuclear Engineering and Technology 54 (2022) 2572–2578

Contents lists available at ScienceDirect

Nuclear Engineering and Technology

journal homepage: www.elsevier.com/locate/net

Original Article

Evaluation of cadmium ratio for conceptual design of a cyclotron-based thermal neutron radiography system

Weng-Sheng Kuo [a, *]

[a] Nuclear Engineering Division, Institute of Nuclear Energy Research, Taiwan, ROC

ARTICLE INFO

Article history:
Received 12 October 2021
Received in revised form
24 December 2021
Accepted 21 January 2022
Available online 4 February 2022

Keywords:
Cadmium ratio
Cyclotron
Thermal neutron radiography system

ABSTRACT

An approximate method for calculating the cadmium ratio of a cyclotron-based thermal neutron radiography system was developed. In this method, the Monte-Carlo code, MCNP6.2, was employed to calculate the neutron capture rates of Au-197, and the cadmium ratio was obtained by computing the ratio of neutron capture rates. From the simulation results, the computed cadmium ratio is reasonably acceptable, and the assumption of ignoring the fast neutron contribution to the cadmium ratio is valid.

1. Introduction

As the decline of number of smaller research reactors in the world, the utilization of cyclotrons as a neutron source has been increased considerably. In 2010, the Union for Compact Accelerator-driven Neutron Sources (UCANS) [1] was formed, devoting to the support of continuous development of small accelerator-driven neutron sources worldwide and promoting the exchange and sharing of information on science, technology and application related to the neutron sources.

The application of cyclotrons, in addition to the conventional radioisotope production, includes medical use (e.g., Boron Neutron Capture Therapy), industrial use (e.g., neutron imaging in fast neutron radiography, thermal neutron radiography, soft error test, etc.), scientific research (such as Small Angle Neutron Scattering). Since year 2020, Institute of Nuclear Energy Research (INER) has also initiated the extension of its TR30/15 compact cyclotron to the area of neutron imaging, starting from the design and built-up of a thermal neutron radiography (TNR) system, followed by a fast neutron radiography facility for soft error tests. Right now, a conceptual design of the TNR system was completed, and a detailed design is ongoing.

In designing the TNR system, the most important parameters [2–4] to be considered are (1) high thermal neutron flux at the collimator exit, (2) high cadmium ratio, (3) low gamma-ray intensity, and (4) large imaging area. The thermal neutron flux and the gamma-ray intensity can be evaluated by computation; whereas, the cadmium ratio is generally measured by taking a neutron activation analysis on a metal foil (mainly gold) at the end of collimator. Here is the dilemma. The TNR system should be set up first prior to measuring the cadmium ratio; but to carry out and optimize the system design, the cadmium ratio should also be determined. Therefore, this paper focuses on the evaluation of cadmium ratio by an approximate yet acceptable calculation method using MCNP6.2 [5], rather than literally taking the neutron activation analysis. Section 2 describes the conceptual design of INER's cyclotron-based TNR system. Section 3 describes the approach to formulating the cadmium ratio equation. Section 4 provides the results of calculation and discussion. Finally, Section 5 gives the conclusion with a recommended future work.

2. Conceptual design of an INER's cyclotron-based TNR system

The INER's TR30/15 cyclotron was designed by TRIUMF (TRI-University Meson Facility, Canada's Particle Accelerator Center) and installed at INER in 1993 by EBCO Inc. (now Advanced Cyclotron Systems Inc.), Canada. Originally operating in a dual mode by accelerating protons (with energy range of 15–30 MeV) and deuterons (with energy range of 7.5–10 MeV), the TR30/15 cyclotron suffered from the malfunctioning of the RF resonator and the dual mode was replaced by the proton mode in 2017. In addition, the

* No. 1000, Wenhua Rd, Jiaan Village, Longtan District, Taoyuan City, 32546, Taiwan, ROC.
E-mail address: wskuo@iner.gov.tw.

https://doi.org/10.1016/j.net.2022.01.021

proton beam capacity was upgraded in 2004–2007 from 0.5 mA to 1 mA. Fig. 1 shows the appearance of INER's TR30/15 cyclotron, and Table 1 lists the machine parameters.

For the thermal neutron radiography system, the target station (including a Be-9 target, and a reflector/moderator cube made of high-density polyethylene [HDPE]) is to be installed in one target irradiation room. Protons come from an extension beam which is extended into the reflector/moderator cube, and bombard the Be-9 target right at the exit of beam line, with a piece of Copper attached behind the Be-9 target as a cooling mechanism. A square opening is located in the HDPE reflector/moderator, a little lower than the Be-9 target; thermal neutrons are introduced from the reflector/moderator block, and then fed through a collimator into a neutron imaging room in a basement directly below the target irradiation room. The collimator is made of HDPE containing 10 wt% boron as B_4C. In addition, a small piece of Bi is installed above the inlet aperture of collimator as a gamma filter. This downward design of the TNR system is due to the limited space in the target irradiation room and the fact that most of the neutrons are forwardly oriented, as protons hit the target in a head-on collision. Table 2 provides the beam tube data and the beam profile parameters. Figs. 2–5 show schematic views of the INER's TNR system, and some major design parameters are listed in Table 3. As shown in the figures, the reflector/moderator is separated into several components for ease of assembling and flexibility in design.

Table 1
Machine parameters of INER's TR30/15 cyclotron.

Particle	H^-
Energy (MeV)	15–30
Extracted Beam (μA)	1000
RF	
Dee voltage (kV)	50
Frequency (MHz)	73.129
Harmonic number	4
Amplifier power (kW)	100
Ion Source	H^- cusp type
Output current (mA)	10
Injection Optics	EBSQQ† + Pulser
Beam Transmission (@ 0.3 mA)	33%
Vacuum (torr)	$<5 \times 10^{-7}$
Magnet	4-sector radial ridge
Beam Lines	4
Beam exit ports	13

Table 2
Beam tube data and beam profile parameters.

Beam Tube	
Material	Al-6061
Inner diameter	9.59 cm
Thickness	0.285 cm
Height	150.0 cm
Beam Profile	
Effective diameter of proton beam	2.0 cm
FWHM‡	1.06 cm

3. Computing cadmium ratio

The cadmium ratio is defined as the ratio of the activity of a bare sample to the activity of a Cadmium covered sample [6]. Normally, the neutron detector is an activation foil and the response is the activity of that foil. Gold is mostly used as the activation foil because it has excellent properties as a capture standard, and sample preparation is very easy since gold is stable, monoisotopic* and easy to fabricate.

Eq. (1) defines the cadmium ratio (R_{CD}), wherein A_{bare} is the activity of a bare gold foil and A_{CD} is the activity of the gold foil covered by cadmium.

$$R_{CD} = \frac{A_{bare}}{A_{CD}}. \quad (1)$$

Assuming that the irradiation time is infinite and the decay time after exposure is the same for both the bare and cadmium-covered condition, Eq. (1) can be reduced to:

$$R_{CD} = \frac{\int_0^\infty \sigma_\gamma(E)\phi(E)dE}{\int_{E_c}^\infty \sigma_\gamma(E)\phi(E)dE} \quad (2)$$

where σ_γ (E) is the microscopic neutron capture cross section of Au-197 at energy E, $\phi(E)$ is the neutron flux at energy E, and E_c is the cadmium cutoff energy, which is normally set as 0.5 eV. It is worth

Fig. 1. Appearance of INER's TR30/15 cyclotron.

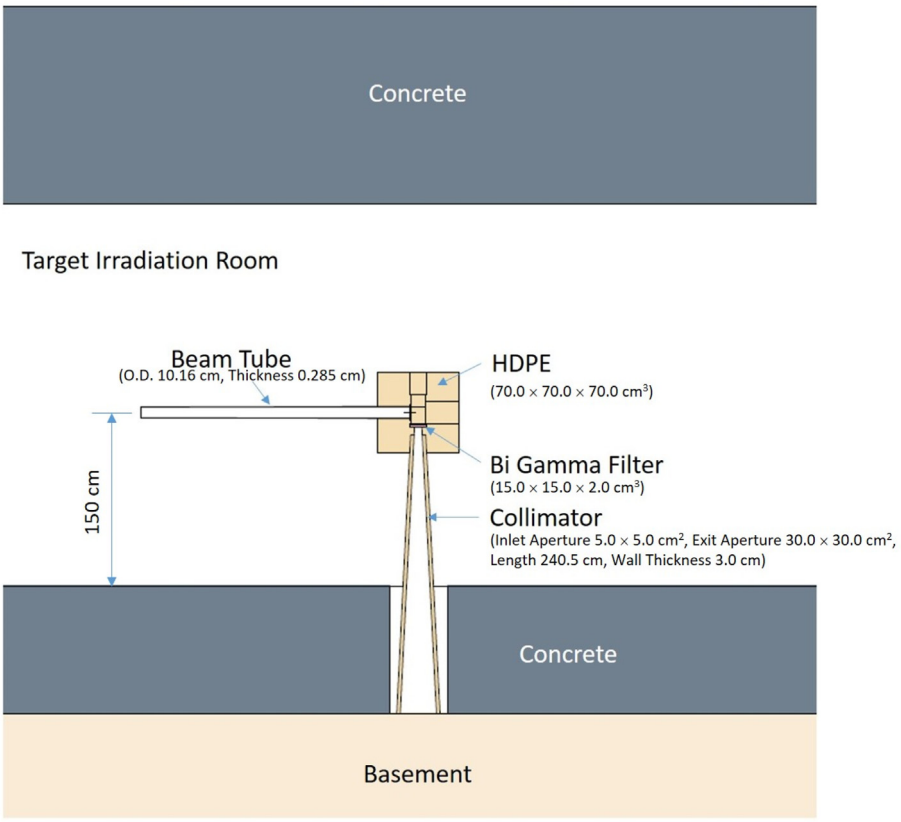

Fig. 2. Side view of TNR system.

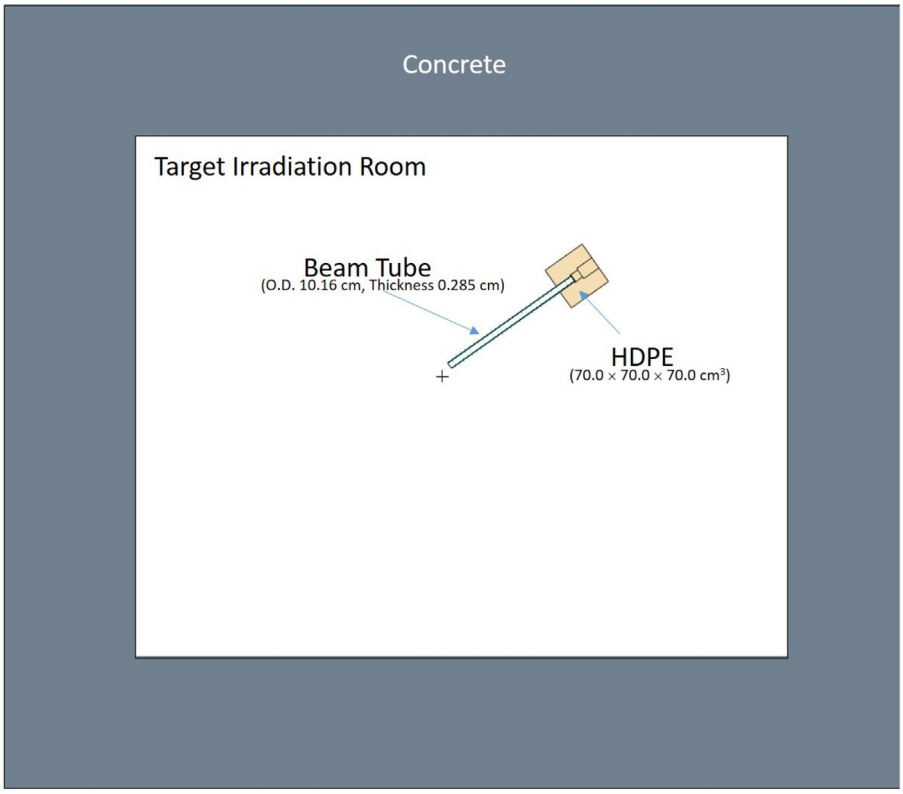

Fig. 3. Top view of TNR system.

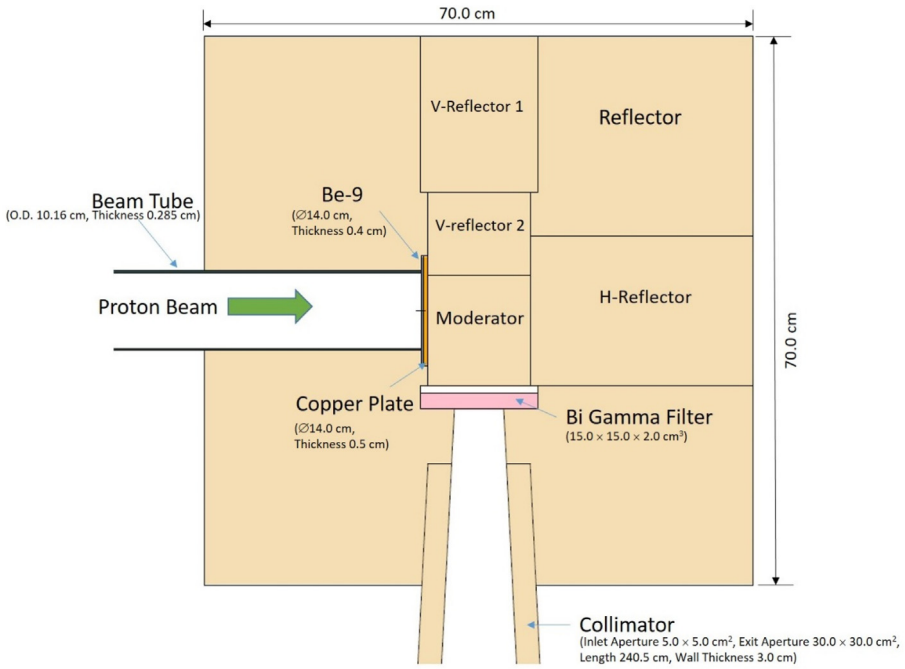

Fig. 4. Partially exploded side view of TMR system.

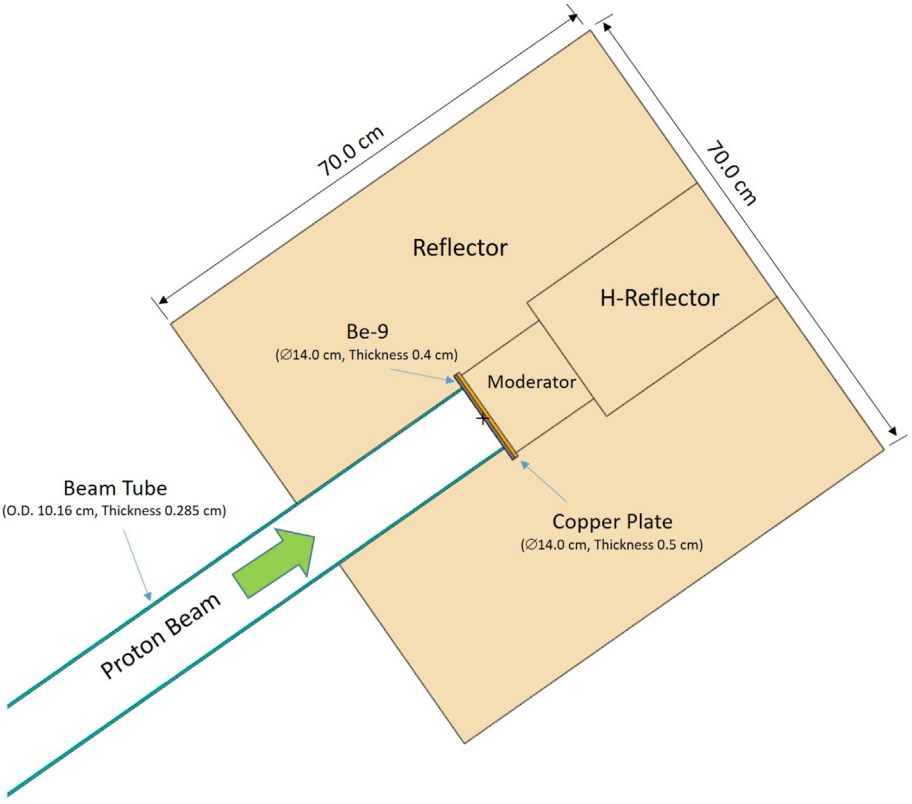

Fig. 5. Partially exploded top view of TNR system.

noting that Eq. (2) is formed by assuming that neutrons with energy less than E_c are completely absorbed by the cadmium cover.

Fig. 6 and Fig. 7 illustrate the microscopic neutron capture cross section of Au-197 and Cd-113, respectively [7]. In Fig. 6, E_c lies just beyond the first absorption peak, and before entering into the resonance absorption region. As shown in Fig. 7, the neutron capture cross section of Au-197 drops significantly compared to the thermal-energy range (at least 10 times lower than the cross

Table 3
Design parameters of TNR system.

Target	
Material	Be-9
Size	Diameter: 14.0 cm, Thickness: 0.4 cm
Reflector/Moderator	
Material	HDPE
Size	70 × 70 × 70 cm^3
Cooling Mechanism	
Material	Cu
Size	Diameter: 14.0 cm, Thickness: 0.5 cm
Gamma Filter	
Material	Bi
Size	15.0 × 15.0 × 2.0 cm^3
Collimator	
Material	HDPE + 10%B
Inlet aperture	5.0 × 5.0 cm^2
Exit aperture	30.0 × 30.0 cm^2
Wall thickness	3.0 cm
Length	240.5 cm

*Au-197 is the only stable isotope in gold.
†E: Einzel lens, B: Buncher, S: Solenoid, Q: Quadruple.
‡FWHM: Full Width at Half Maximum.

section around 1 eV, and much more for neutron energy less than 1 eV) when neutron energy is larger than 10^{-2} MeV (or 10 keV), which is just out of the resonance absorption range and is denoted as E_{ep} in the figure. Therefore, by ignoring the contribution to the neutron capture rate of neutrons with energy larger than 10 keV, Eq. (2) is simplified to:

$$R_{CD} = \frac{\int_0^{E_c}\sigma_\gamma(E)\phi(E)dE + \int_{E_c}^{E_{ep}}\sigma_\gamma(E)\phi(E)dE + \int_{E_{ep}}^{\infty}\sigma_\gamma(E)\phi(E)dE}{\int_{E_c}^{E_{ep}}\sigma_\gamma(E)\phi(E)dE + \int_{E_{ep}}^{\infty}\sigma_\gamma(E)\phi(E)dE} \approx \frac{\int_0^{E_c}\sigma_\gamma(E)\phi(E)dE + \int_{E_c}^{E_{ep}}\sigma_\gamma(E)\phi(E)dE}{\int_{E_c}^{E_{ep}}\sigma_\gamma(E)\phi(E)dE}. \quad (3)$$

In this paper, the cadmium ratio is evaluated using Eq. (3), and the neutron capture rates are calculated by the Monte Carlo neutron transport code MCNP6.2, due to the complexity of geometry, as well as the general popularity and reliability of the code in nuclear industries.

An MCNP model was setup using the ENDF/B-VII.1 continuous neutron cross section data and the default proton cross section data. The simulation was performed under an irradiation condition of proton energy of 18 MeV and proton current of 50 μA. The proton beam was simulated as a beam source in MCNP, with protons bombarding the Be-9 target at right angle, and a Gaussian distribution (FWHM of 1.06 and an effective diameter of 2.0 cm, as shown in Table 2) across the surface of Be-9. To evaluate the cadmium ratio, the neutron fluxes in a small air slab on an exit plane of collimator were computed (with the F4 tally) and then the neutron capture rates of Au-197 were calculated from the integration of neutron fluxes with capture cross sections of Au-197 (with the FM multiplier). Notably, there is no need to include Au-197, Cadmium cover, and a neutron detector in the simulation; this is a special tallying function in MCNP. In addition, as shown in Eq. (2) and Eq. (3), the time effect was totally omitted, and thus, the timing (e.g., from proton pulse) to the detection time was irrelevant in this simulation.

4. Results and discussion

The cadmium ratio calculated by Eq. (3) is 2.998 ± 4.73%, which ignores the contribution of fast neutron capture rate. In comparison, the cadmium ratio obtained from Eq. (2) is 2.992 ± 4.72%, proving that the assumption of ignoring the fast contribution is valid. Given that the thermal neutron radiography system is only a conceptual design and no optimization has been done yet, the calculated cadmium ratio is reasonably acceptable. Furthermore, it is interested in checking the statistical convergence of calculation. Fig. 8 shows the calculated cadmium ratio as a function of no. of sampled histories, Fig. 9 presents the calculated neutron capture rate (the error bars in the thermal and fast neutron range are negligibly smaller than the error bars in the epithermal neutron range) as a function of no. of sampled histories, and Fig. 10, the

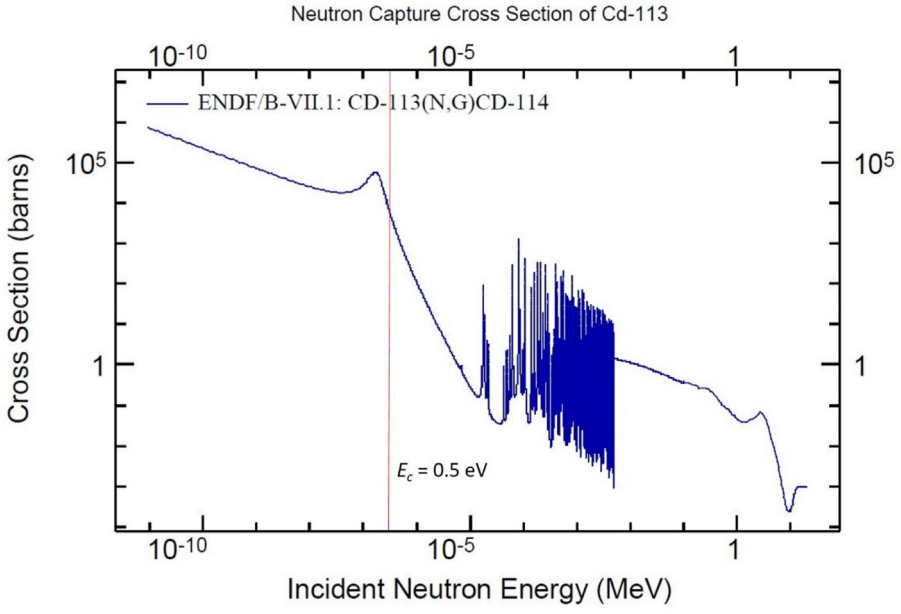

Fig. 6. Neutron capture cross section of Cd-113 (ENDF/B-VII.1).

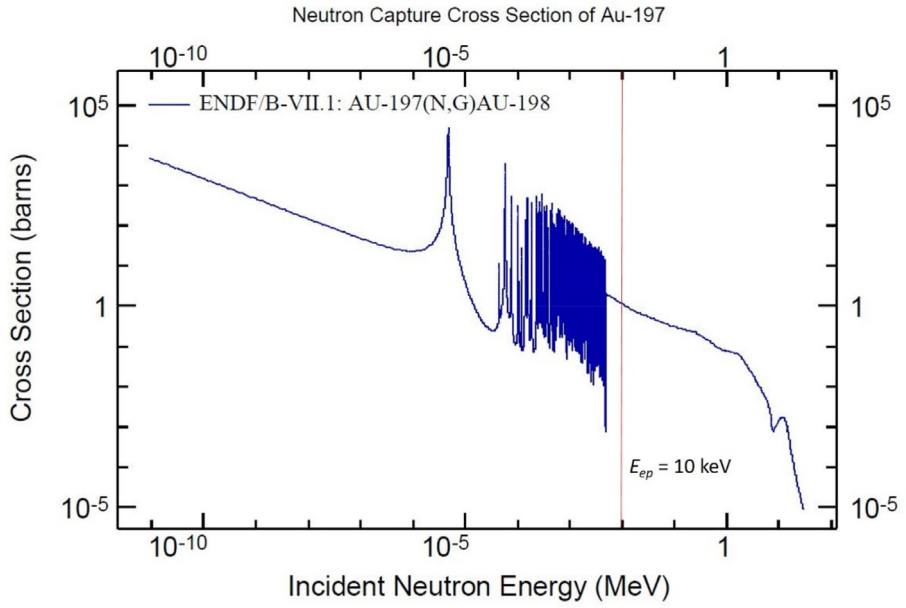

Fig. 7. Neutron capture cross section of Au-197 (ENDF/B-VII.1).

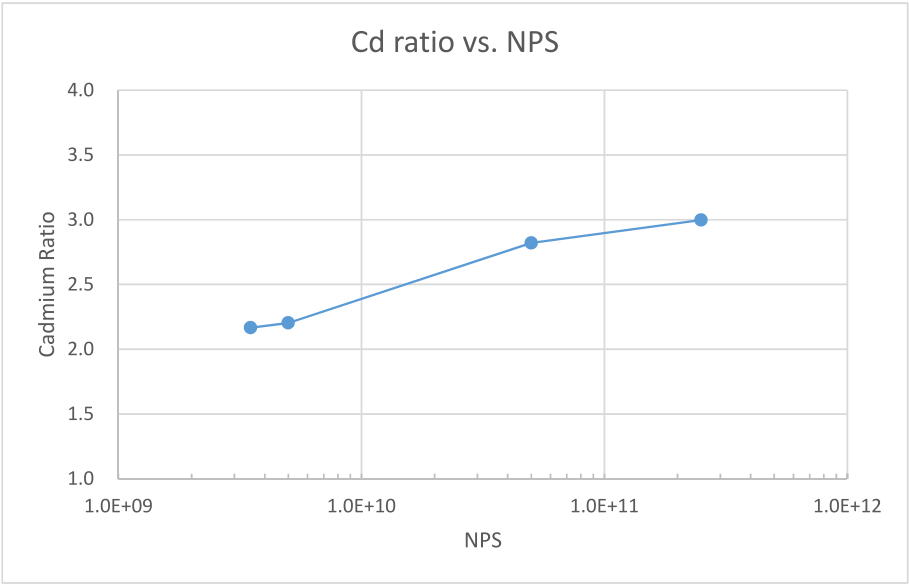

Fig. 8. Cadmium ratio as a function of no. of histories (NPS).

relative statistical error of neutron capture rate as a function of no. of sampled histories. As shown in the Figures, the cadmium ratio increases as the no. of sampled histories to a stably converged value, and the captures rates in the thermal and fast neutron range converge rather faster than the captures rate in the epithermal neutron range, which shows that the capture rate in the epithermal neutron range dominates the calculation of cadmium ratio.

5. Conclusion

In this paper, an approximate method was developed to evaluate the cadmium ratio for a conceptual design of INER's TNR system. The evaluation was totally based on the MCNP calculations, without literally carrying out the neutron activation analysis. The calculated cadmium ratio is reasonably acceptable and the assumption of ignoring the fast neutron contribution in calculating the cadmium ratio is valid. In addition, the neutron capture rate in the epithermal neutron range plays a dominant role in calculating the cadmium ratio. Currently, a detailed design of INER's TNR system is in process. In the near future, when the INER's TNR system is built up, this cadmium ratio calculation method will be benchmarked against the real measurement from the neutron activation analysis, specifically for the assessment of validity of Eq. (3) as compared to Eq. (2). In addition, the neutron spectrum at the exit plane of collimator will also be computed and benchmarked against a real measurement (e.g., Bonner sphere detector system), for better understanding of the performance of the system. Finally, this cadmium ratio calculation method can be used as an evaluation tool for design of any thermal neutron system as well.

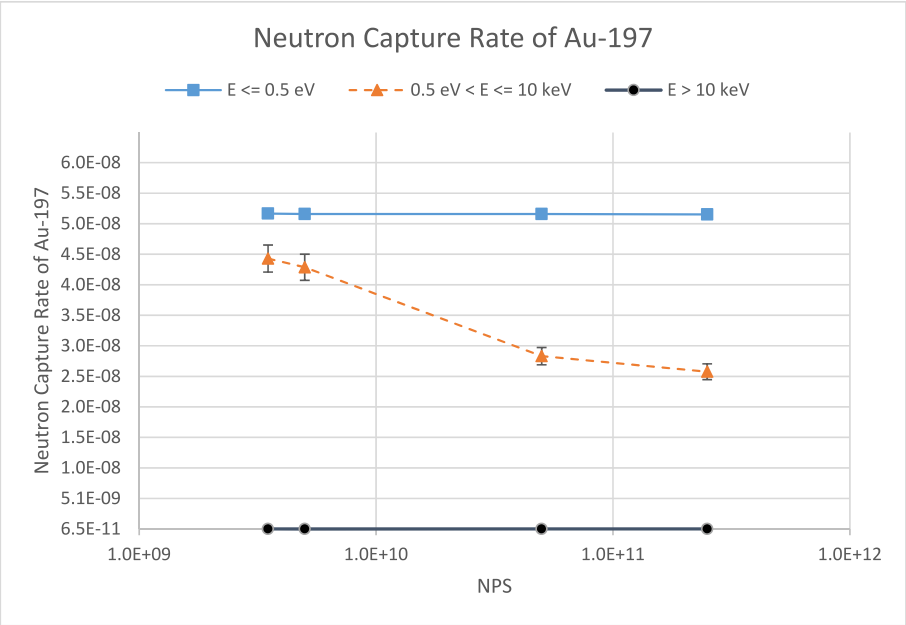

Fig. 9. Neutron capture rate as a function of no. of histories (NPS).

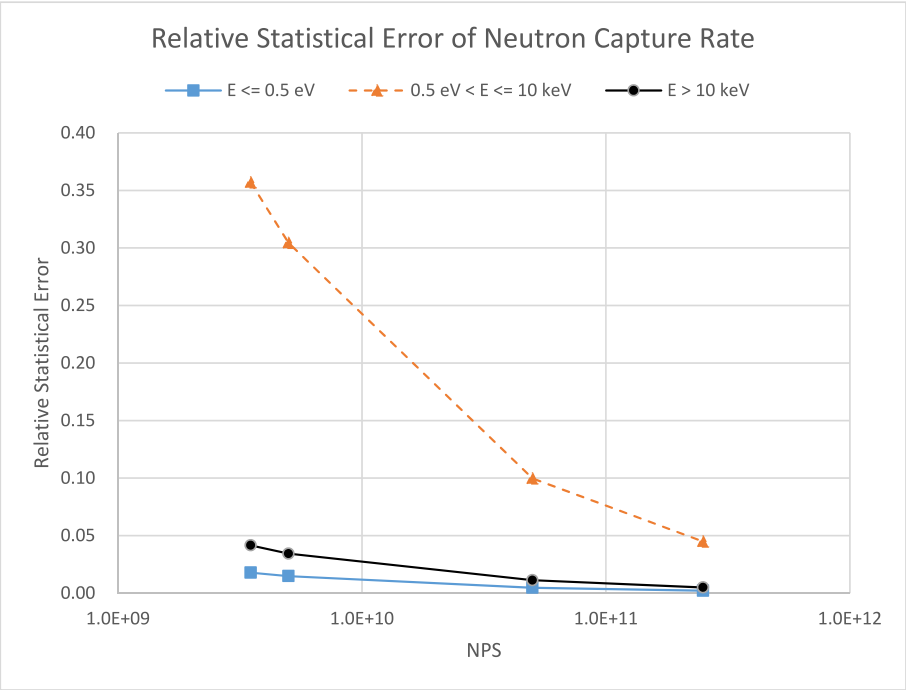

Fig. 10. Relative statistical error of neutron capture rate.

Declaration of competing interest

The authors declare that they have no known competing financial interests or personal relationships that could have appeared to influence the work reported in this paper.

6. References

[1] UCANS. http://www.ucans.org.
[2] J.C. Domanus, Practical Neutron Radiography, 1992, ISBN 0792318609.
[3] IAEA, Use of Neutron Beams for Low and Medium Flux Research Reactors: Radiography and Materials Characterization, IAEA-TECDOC-837, 1993.
[4] M.A. Abdou Mandour, et al., Characterization and application of the thermal neutron radiography beam in the Egyptian second experimental and training research reactor (ETRR-2), Science and Technology of Nuclear Installations 2007 (2007), 24180.
[5] Christopher J. Werner, "MCNP User's Manual Code Version 6.2,", LA-UR-17-29981, Los Alamos National Laboratory, 2017.
[6] Dante Marco Zangirolami, et al., Thermal and epithermal neutron fluence rates in the irradiation facilities of the TRIGA IPR-R1 nuclear reactor, Braz. J. Phys. 40 (1) (March, 2010).
[7] ENDF. https://www-nds.iaea.org/exfor/endf.htm.